Upregulation of insulin receptor substrate-2 in pancreatic β cells prevents diabetes

Anita M. Hennige, … , Mahmud Mossa-Basha, Morris F. White

Article   **Metabolism**

The insulin receptor substrate-2 (Irs2) branch of the insulin/IGF signaling system coordinates peripheral insulin action and pancreatic β cell function, so mice lacking *Irs2* display similarities to humans with type 2 diabetes. Here we show that β cell–specific expression of *Irs2* at a low or a high level delivered a graded physiologic response that promoted β cell growth, survival, and insulin secretion that prevented diabetes in *Irs2*$^{-/-}$ mice, obese mice, and streptozotocin-treated mice; and that upon transplantation, the transgenic islets cured diabetes more effectively than WT islets. Thus, pharmacological approaches that promote *Irs2* expression in β cells, especially specific cAMP agonists, could be rational treatments for β cell failure and diabetes.

Find the latest version:

https://jci.me/18581/pdf

Upregulation of insulin receptor substrate-2 in pancreatic β cells prevents diabetes

Anita M. Hennige,[1] Deborah J. Burks,[1] Umut Ozcan,[2] Rohit N. Kulkarni,[2] Jing Ye,[1] Sunmin Park,[1] Markus Schubert,[1] Tracey L. Fisher,[1] Matt A. Dow,[1] Rebecca Leshan,[1] Mark Zakaria,[1] Mahmud Mossa-Basha,[1] and Morris F. White[1]

[1]Howard Hughes Medical Institute, Joslin Diabetes Center, Harvard Medical School, Boston, Massachusetts, USA
[2]Research Division, Joslin Diabetes Center, Harvard Medical School, Boston, Massachusetts, USA

The insulin receptor substrate-2 (Irs2) branch of the insulin/IGF signaling system coordinates peripheral insulin action and pancreatic β cell function, so mice lacking *Irs2* display similarities to humans with type 2 diabetes. Here we show that β cell–specific expression of *Irs2* at a low or a high level delivered a graded physiologic response that promoted β cell growth, survival, and insulin secretion that prevented diabetes in *Irs2⁻/⁻* mice, obese mice, and streptozotocin-treated mice; and that upon transplantation, the transgenic islets cured diabetes more effectively than WT islets. Thus, pharmacological approaches that promote *Irs2* expression in β cells, especially specific cAMP agonists, could be rational treatments for β cell failure and diabetes.

Introduction

Diabetes mellitus arises from dysregulated glucose sensing or insulin secretion (mature onset diabetes of youth, or MODY), autoimmune-mediated β cell destruction (type 1), or insufficient compensation for peripheral insulin resistance (type 2) (1). As insulin resistance develops, type 2 diabetes is avoided by expanding functional β cells that secrete sufficient insulin quickly enough to maintain glucose homeostasis. Diet, acute or chronic stress, and obesity are major determinants of peripheral insulin sensitivity, and age exacerbates these environmental effects. While it is clear that insulin resistance and β cell dysfunction contribute to type 2 diabetes, there is considerable debate regarding the relative importance of these two abnormalities (2, 3). Studies with humans and rodents reveal a tightly controlled inverse relationship between insulin sensitivity and insulin secretion, suggesting that a feedback mechanism balances β cell function with the prevailing level of peripheral insulin sensitivity (3). When β cell compensation fails, glucose intolerance and type 2 diabetes develop, but the mechanisms involved and whether they are linked at the molecular level are unknown (4).

How insulin sensitivity influences insulin secretion is poorly understood. Recent work with transgenic mice suggests that β cell function is regulated by insulin and IGF signaling (5). The receptors for insulin and IGF1 promote phosphorylation of the insulin receptor substrates, Irs1 and Irs2, which engage various downstream pathways, including the Grb2/Sos → ras and the PI3K → Akt cascades (6–8). Although these pathways were originally described in heterologous cell lines and peripheral tissues, recent work suggests that they play a central role in β cell function. Insulin action and secretion are closely linked at the molecular level through the Irs2 branch of the insulin/IGF signaling cascade (9, 10). Global disruption of *Irs2* causes peripheral insulin resistance that is compensated for by relative hyperinsulinemia early in life; however, *Irs2⁻/⁻* mice progress toward diabetes as β cell mass decreases and insulin secretion fails (9, 11–13). By contrast, peripheral insulin resistance caused by obesity or by disruption of *Irs1* is compensated for, at least in part, by expansion of β cell mass (9, 14). Disruption of the receptors for insulin or IGF1 in β cells impairs first-phase insulin secretion, which contributes to glucose intolerance (11–13). Together these results suggest that the Irs2 branch of the insulin/IGF signaling pathway is essential for β cell function throughout life.

Identifying a single genetic defect that causes insulin resistance and β cell failure has been difficult to accomplish, leading many investigators to conclude that ordinary type 2 diabetes is a polygenic disorder (3). By contrast, disruption of *Irs2* in mice reveals a single defect that causes both insulin resistance and β cell dysfunction that culminates in diabetes (9, 15). Mutations in *IRS2* are unusual and probably not associated with common type 2 diabetes in people (16). However, genetic polymorphism or environmental stress that compromises Irs2 function or diminishes its downstream signals might explain the heterogeneity of common type 2 diabetes in terms of a defined signaling cascade.

Since Irs2 plays an important role in β cell function, we reasoned that its upregulation might prevent diabetes under conditions that cause insulin resistance or physiological stress. To test this hypothesis, we generated transgenic mice expressing *Irs2* at a low or a high level in β cells under the control of the rat insulin II promoter (rip). Our results show that *Irs2* expression prevents diabetes that results from a variety of causes.

Methods

Generation of rip→Irs2 transgenic mice. A 668-bp rip constructed in the pSP72 vector was kindly provided by Mark Magnuson (Vanderbilt University, Nashville, Tennessee, USA). The FLAG tag sequence was added to the 3′ end of mouse *Irs2* by PCR and the tagged cDNA was then inserted directly after the rip promoter using the NotI/HindIII sites. A linearized DNA fragment containing the *rip-Irs2* transgene was excised and microinjected into fertilized eggs of C57BL/6 mice according to standard techniques by the Beth Israel Deaconess Transgenic Mouse Facility (Boston, Massachusetts, USA). Germline transmission was confirmed by Southern blotting. Founders were bred with C57BL/6 mice and maintained on this pure background. Routine genotyping was executed by PCR using primers derived from the FLAG tag and an internal *Irs2* sequence. Experiments were performed on mice of line 9 and line 13 (*rip9→Irs2* and *rip13→Irs2*) and their nontransgenic littermates. To obtain mice with a homozygous knockout for *Irs2* that were *rip-Irs2* transgene–positive (*Irs2−/−:rip→Irs2*), we bred *Irs2+/−:rip→Irs2* animals. All procedures were performed with male mice on a pure C57BL/6 background and in accordance with the policies of the Institutional Animal Care and Use Committee of Beth Israel Deaconess Medical Center and Harvard School of Public Health.

Pancreatic insulin content. Pancreata from euthanized mice were homogenized and protein was extracted twice overnight at –20°C in acid-ethanol and stored at –20°C. The extracts were combined and the immunoreactive insulin levels were measured by ELISA (Crystal Chem Inc., Downers Grove, Illinois, USA) with mouse insulin as a standard.

Min6 cell culture and analysis. Min6 cells were used between passages 19 and 30, and grown in high-glucose DMEM containing 15% (vol/vol) heat-inactivated FBS, 50 μM β-mercaptoethanol, 50 U/ml penicillin, and 10 μg/ml streptomycin. Min6 β cells were cultured in a humidified atmosphere at 37°C with 5% CO_2. At 80% confluence, cells were washed with PBS and incubated in serum-free medium for 8 hours without compound or with exendin-4 or dibutyl-cAMP. After the treatment, cells were harvested in ice-cold PBS and lysed in 20 mM Tris (pH 7.4) containing 2 mM EDTA, 137 mM NaCl, 1% NP-40, 10% glycerol, and 12 mM β-glycerol phosphate, 1mM PMSF, and 10 mg/μl leupeptin and aprotinin. After 30 minutes on ice, the lysates were centrifuged for 10 minutes at 14,000 *g* at 4°C. After determining protein content, equal amounts of total protein (200 μg) were incubated with anti-Irs2 antibody, precipitated on immobilized protein G, resolved by SDS-PAGE, and immunoblotted with anti-Irs2.

Islet preparation. Isolated islets were obtained by collagenase P digestion of pancreata removed from WT, *Irs2−/−*, *rip9→Irs2*, *rip13→Irs2*, *Irs2−/−:rip9→Irs2*, and *Irs2−/−:rip13→Irs2* mice (17). Overnight-fasted mice, aged 6–10 weeks, were anesthetized by intraperitoneal injection with Avertin (1.0 ml/40 g body wt). About 2.0 ml of a collagenase solution (0.8 mg/ml in RPMI 1640) was injected into the bile duct to inflate the pancreas. After the pancreas was removed, the tissue was incubated at 37°C for 30 minutes to complete the digestion. Following digestion, islets were selected from the media and washed once in RPMI with 10% FBS, then twice in RPMI without FBS. Following isolation, islets were either suspended in CMRL 1066 supplemented with 10% FBS and antibiotics and then cultured in 37°C in a CO_2 incubator for further experiments, or quickly frozen in liquid nitrogen for protein extraction, SDS-PAGE, and immunoblotting. In some experiments, 200 islets were pelleted for mRNA isolation and GeneChip analysis.

RNA isolation, cRNA preparation, and array hybridization. WT mice aged 4–6 weeks displaying normal fasting and random-fed insulin and blood glucose levels were starved overnight, anesthetized in the morning by intraperitoneal injection with Avertin (1.0 ml/40 g body wt), and used for the isolation of skeletal muscle (300 mg), liver (100 mg), adipose tissue (150 mg), or brain (100 mg). Total RNA was isolated using Trizol (Invitrogen Corp., Chicago, Illinois, USA) and purified with RNeasy (Qiagen Inc., Los Angeles, California, USA), and mRNA was isolated using Oligotex (Qiagen Inc.). The SuperScript Choice System (Invitrogen Corp.) was used to prepare cDNA. Labeled cRNA (15 μg) was made with the MEGAscript T7 high-yield transcription kit (Ambion Inc., Houston, Texas, USA), fragmented, and hybridized to Affymetrix murine genome (MG) U74v2 arrays A, B, and C according to the GeneChip Expression Analysis manual (Affymetrix Inc., San Francisco, California, USA). Islet samples were prepared using the GeneChip Eukaryotic Small Sample Target Labeling Assay, version 1. Approximately 1 μg of total RNA was isolated from about 200 islets collected from WT, *rip13→Irs2*, or *Irs2−/−:rip13→Irs2* mice at 6 weeks of age. Approximately 100 mg of RNA was amplified to obtain 15 μg of cRNA for hybridization. All samples were hybridized and scanned at the Massachusetts Institute of Technology Center for Cancer Research/Howard Hughes Medical Institute Biopolymers Laboratory. The primary data was analyzed with Affymetrix GeneChip (version 5). The trimmed mean signals of the probe arrays were scaled to a value of 500. GeneSpring (version 5.0; Silicon Genetics, Redwood City, California, USA) was used to annotate the results and normalize each chip and gene — except those marked absent — until the medians converged.

Analysis of signaling proteins in isolated islets. Isolated islets incubated for 12 hours in CMRL 1066 containing 10% FCS were used to determine total protein levels and/or the phosphorylation states of Akt1/2, Foxo1, Erk1/2, and cleaved caspase-3. Subsequently, the islets were starved for 3 hours in CMRL 1066 without serum. The islets were then cultured in the absence or presence of IGF1 (100 nM) for 20 minutes. The islet lysates were boiled for 5 minutes in SDS sample buffer and resolved by 12% SDS-PAGE for 2–3 hours at 100 V and transferred to a nitrocellulose membrane for immunoblotting. The membranes were incubated overnight with primary antibodies at 4°C (Cell Signaling Technology Inc., Beverly, Massachusetts, USA), washed with TBST for 30 minutes, incubated for 1 hour with HRP-conjugated secondary antibodies, and finally washed thoroughly and subjected to enhanced chemiluminescence (NEN Life Science Products Inc., Boston, Massachusetts, USA).

Islet morphology and immunohistochemistry. For immunohistochemistry, pancreatic sections were fixed for 16 hours in 4% paraformaldehyde and then transferred to PBS until embedding in paraffin as previously described (18). Following rehydration and permeabilization with 1% Triton X-100, sections were incubated overnight at 4°C with antibodies targeted to specific proteins of interest as previously described (18). Transgenic Irs2 was detected with anti-FLAG (Eastman Kodak Co., New Haven, Connecticut, USA), insulin was detected with guinea pig anti-insulin (Zymed Laboratories Inc., South San Francisco, California, USA), glucose transporter-2 (Glut2) was detected with rabbit anti-Glut2 antibodies (Calbiochem-Novabiochem Corp., San Diego, California, USA), and glucagon was detected with anti-glucagon (Zymed Laboratories Inc.). The anti-FLAG antibody was detected with secondary antibodies conjugated to cyanine. The other antibodies were detected with fluorescene-tagged secondary antibodies. To minimize variability between different sections, the staining procedures for the sections were performed in parallel with the same batches of solutions and antisera. In addition, the same incubation times for fixation, permeabilization, blocking, and exposure to antisera were strictly used for all processed sections.

Islet proliferation was estimated by injecting 8-week-old male mice with 100 μg/g body wt BrdU (Roche Molecular Biochemicals, Indianapolis, Indiana, USA), and pancreas sections were analyzed by double staining with anti-insulin and anti-BrdU (Roche Molecular Biochemicals) (18). Apoptotic cells were identified in deparaffinized sections using a rhodamine DNA fragmentation detection assay (Intergen Co., Atlanta, Georgia, USA) (19). For quantification of β cell area, sections were viewed using a Zeiss Axiovert S100 TV microscope (Carl Zeiss Inc., Thornwood, New York, USA) at a magnification of ×10. Cross-sectional area of islets with more than five insulin-positive cells was measured with at least three sections (separated by 200 μm) per animal using

Openlab Image analysis software (Improvision Inc., Lexington, Massachusetts, USA). The results are expressed as the percentage of the total area of each pancreatic section. The ratio of β cells to α cells was calculated from mean insulin- and glucagon-positive cell areas measured by double immunostaining.

Metabolic studies and mouse diet. Mice were fed ad libitum with a standard 9% fat diet (5058; Purina Mills Inc., St. Louis, Missouri, USA) and kept under a light-dark cycle of 12 hours. When stated, mice were weaned on a high-fat diet (45 kcal% fat) or low-fat diet (10 kcal% fat) for 60 days (D12451 and D12450B, respectively; Research Diets, New Brunswick, New Jersey, USA). Glucose levels were sampled from mouse tail bleeds using a Glucometer Elite (Bayer Corp., Elkhart, Indiana, USA). Plasma insulin levels were determined using a competitive ELISA (Crystal Chem Inc.). Glucose tolerance tests were performed on mice after a 16-hour overnight fast. Animals were injected intraperitoneally with D-glucose (2 g/kg), and blood glucose concentrations were determined at indicated times. Glucose-stimulated insulin release was measured in fasted mice injected intraperitoneally with D-glucose (3 g/kg). As indicated, mice were subjected to an intraperitoneal injection of low-dose streptozotocin (40 mg/kg body wt dissolved immediately before administration in 0.1 M citrate buffer, pH 4.5) for 5 consecutive days.

Islet transplantation. Mice were made diabetic by daily injections of streptozotocin for 3 days (100 mg/kg body wt dissolved immediately before administration in 0.1 M citrate buffer, pH 4.5) as previously described (20). Islets used for transplantation were isolated from healthy male 8-week-old mice as described previously using intraductal Liberase (Roche Molecular Biochemicals) perfusion to release islets from the pancreas tissue for manual selection under a stereomicroscope (Stereozoom GZ7; Leica Microsystems Inc., Deerfield, Illinois, USA) (20). Following isolation, islets were kept on ice until transplantation into diabetic mice. Surgery was performed under anesthesia by using a 1:1 mixture of 2,2,2-tribromoethanol and *tert*-amyl alcohol and diluted 1:50 in PBS (pH 7.4). Using a retroperitoneal approach, the capsule of one of the kidneys was incised, and the islets were implanted near the upper pole in 8-week-old male mice. The capsule was cauterized, and the mice were allowed to recover on a heating pad.

Statistical analysis. Results are expressed as mean ± SEM. For comparison between two groups, the unpaired Student *t* test (two tailed) was used when appropriate; *P* values less than 0.05 were considered significant. To quantify the difference between glucose tolerance tests or glucose-stimulated insulin secretion, the area under the curve (AUC) was calculated by the trapezoid rule using SigmaPlot 8.02 (SPSS Inc., Chicago, Illinois, USA). The mean AUC ± SEM was determined from at least five individual curves for each experimental condition reported.
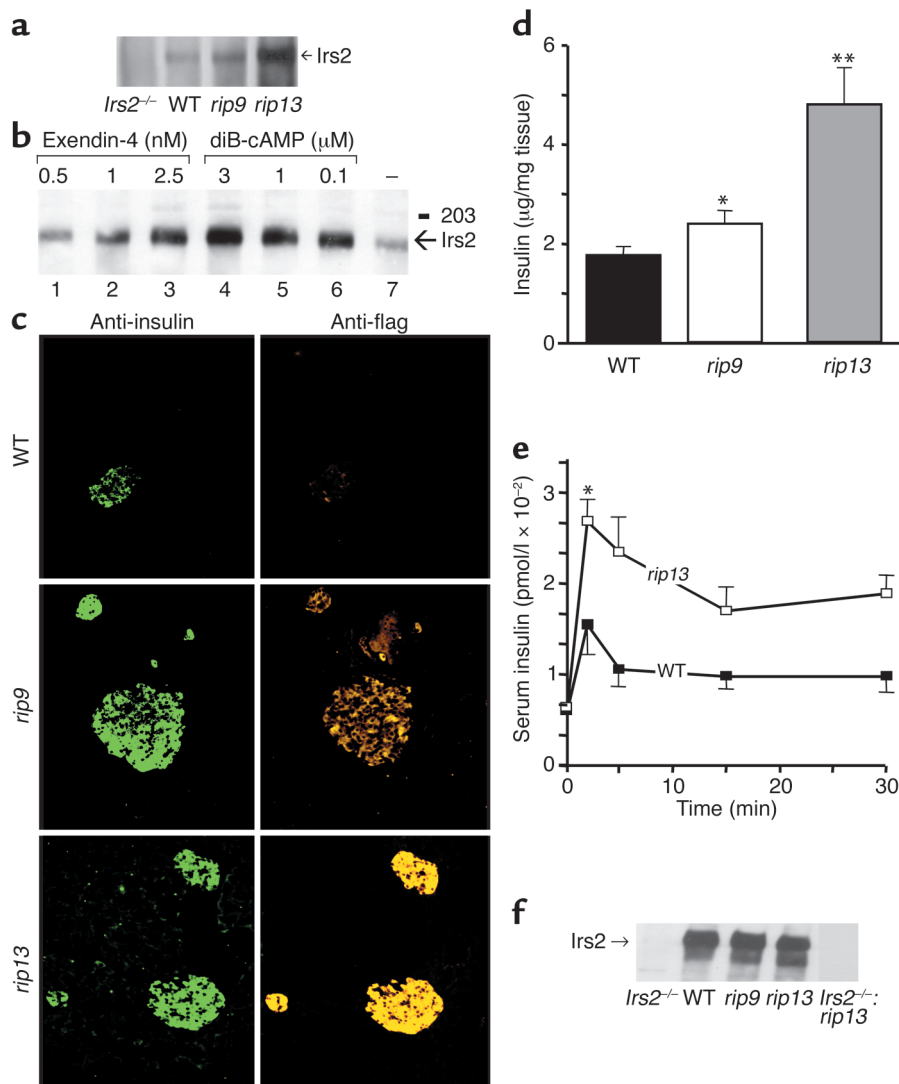
Figure 1

Irs2 protein expression and β cell function. (**a**) Irs2 protein levels measured by specific immunoblotting in Irs2 immunoprecipitates of 200 μg total protein from islet extracts of 4-week-old WT mice, *Irs2*$^{-/-}$ mice, or two lines of transgenic mice (*rip9*$^{→Irs2}$ and *rip13*$^{→Irs2}$). (**b**) Irs2 protein levels measured by specific immunoblotting in Irs2 immunoprecipitates of 200 μg total protein from Min6 cells treated for 8 hours with the indicated concentrations of exendin-4 or dibutyl-cAMP (diB-cAMP) (**c**) Representative WT, *rip9*$^{→Irs2}$, or *rip13*$^{→Irs2}$ pancreas sections immunostained with anti-insulin antibodies (left panel) or anti-FLAG antibodies (right panel) that were detected by cyanine (Irs2) or fluorescein (Insulin) conjugated secondary antibodies, respectively. Original magnification, ×100. (**d**) Pancreatic insulin content per mg total pancreas was measured in acid/ethanol extracts of total pancreas from 6-month-old WT, *rip9*$^{→Irs2}$, and *rip13*$^{→Irs2}$ mice. Data are the mean values ± SEM of five mice per genotype. *$P < 0.05$, **$P < 0.01$. (**e**) Glucose-stimulated insulin release measured in 6-week-old WT and *rip13*$^{→Irs2}$ mice. D-glucose (3 g/kg body wt) was injected intraperitoneally into 16-hour-fasted mice and blood samples were collected at the indicated timepoints. Results are expressed as mean values ± SEM of six WT and six *rip*$^{→Irs2}$ mice (*$P < 0.05$). (**f**) Irs2 protein levels measured by specific immunoblotting in Irs2 immunoprecipitates from hypothalamic extracts of 4-week-old WT, *rip9*$^{→Irs2}$, *rip13*$^{→Irs2}$, *Irs2*$^{-/-}$, or *Irs2*$^{-/-}$:*rip13*$^{→Irs2}$ mice. *rip9*, *rip9*$^{→Irs2}$; *rip13*, *rip13*$^{→Irs2}$.

Results

Upregulation of Irs2 in β cells. To determine whether β cell dysfunction is a pivotal element in the development of diabetes in *Irs2*$^{-/-}$ mice, we generated transgenic C57BL/6 mice expressing a low (*rip9*$^{→Irs2}$) or a high (*rip13*$^{→Irs2}$) level of *Irs2* in pancreatic β cells under the control of rip. Irs2 was measured by specific immunoblotting of islet extracts containing equal amounts of total protein (Figure 1a). Irs2 was detected in WT islet extracts but was undetectable in *Irs2*$^{-/-}$ islets. Concurrent immunoblots revealed twofold and 12-fold increased Irs2 in *rip9*$^{→Irs2}$ and *rip13*$^{→Irs2}$ extracts (Figure 1a), which was similar to that obtained physiologically by activation of the endogenous *Irs2* promoter with functional cAMP response element binding protein (21). Moreover, the relative increase of transgenic Irs2 in islets was comparable to the upregulation of endogenous Irs2 in Min6 β cells treated for 10 hours with exendin-4 or dibutyl-cAMP (Figure 1b).
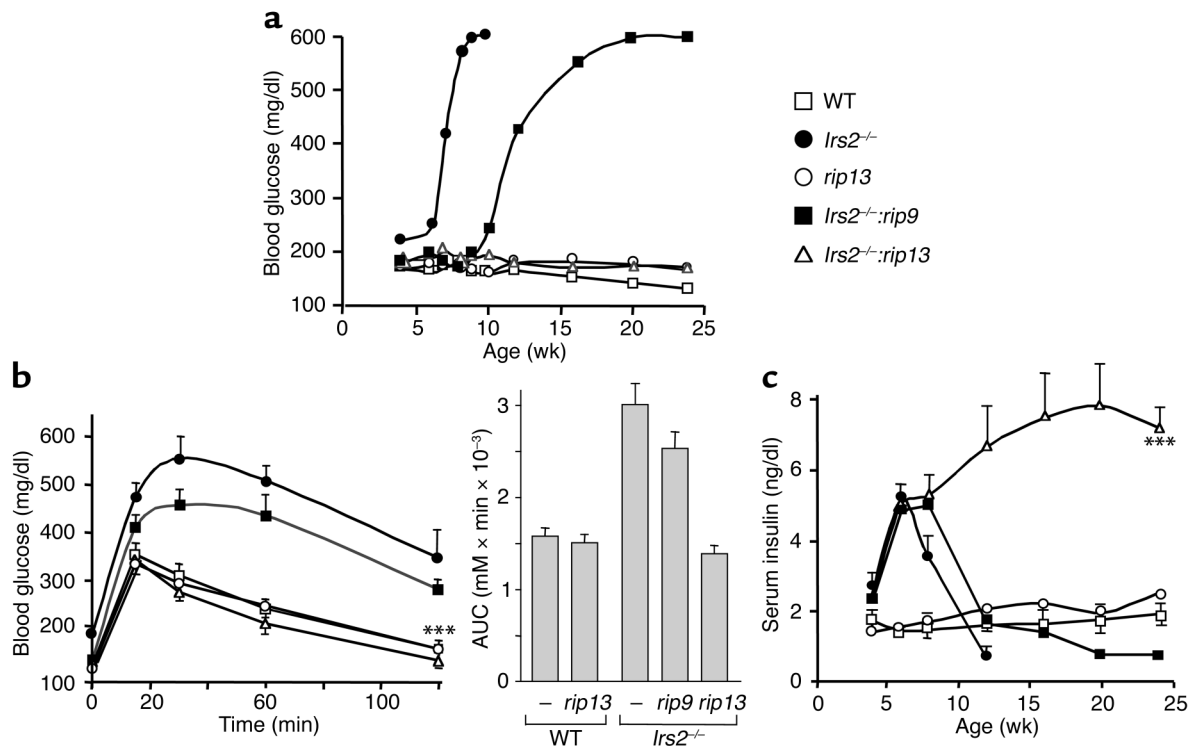
Figure 2

Metabolic effects of *Irs2* overexpression in β cells. (**a**) Blood glucose concentrations were measured from tail bleeds of fed male mice. Values are mean ± SEM obtained from WT, *rip13→Irs2*, *Irs2−/−*, and *rip→Irs2* mice crossed into a C57BL/6 *Irs2−/−* background (*Irs2−/−:rip9→Irs2* and *Irs2−/−:rip13→Irs2*). Data are the mean values ± SEM of four (*Irs2−/−:rip9→Irs2*) to ten (WT, *Irs2−/−*, *rip13→Irs2*, and *Irs2−/−:rip13→Irs2*) mice of the indicated ages. (**b**) Glucose-tolerance tests were performed on 8-week-old fasted mice following intraperitoneal loading with 2 g D-glucose per kg body wt. Blood samples were taken at the timepoints indicated and glucose was determined as described. Results are mean ± SEM of four to ten mice (***P < 0.001, *Irs2−/−* vs. *Irs2−/−:rip13→Irs2*). (**c**) Random-fed serum insulin levels (mean values ± SEM, ***P < 0.001) measured by ELISA.

Our transgenic production strategy incorporated a FLAG tag at the C terminus of Irs2 to facilitate immunostaining. Pancreas sections immunostained with anti-FLAG antibodies revealed that recombinant Irs2 protein was restricted to the insulin-positive β cells in *rip9→Irs2* and *rip13→Irs2* islets (Figure 1c). Moreover, the pancreatic insulin content increased 1.3-fold in *rip9→Irs2* mice and 2.7-fold in *rip13→Irs2* mice, revealing a dose effect of *Irs2* expression on β cell insulin content (Figure 1d). During an intraperitoneal glucose challenge, insulin secretion during the first 30-minute interval was threefold higher in *rip13→Irs2* mice than in WT mice (AUC WT: 1,880 ± 50 nmol × min/l; AUC *rip13→Irs2*: 5,440 ± 50 nmol × min/l) (Figure 1e). However, glucose homeostasis was normal in *rip13→Irs2* mice from birth until the experiment was terminated after 24 weeks, as fasting glucose never fell below 79 ± 3 mg/dl and fed glucose never rose above 159 ± 6 mg/dl. Both transgenic mouse lines displayed normal fertility, growth, and adiposity, and had normal life spans (data not shown). Irs2 protein was never detected in hypothalamus (Figure 1f), nor was it detected in liver, muscle, or adipose tissues (data not shown).

Irs2 in β cells prevents diabetes in Irs2−/− mice. Male C57BL/6 *Irs2−/−* mice developed hyperglycemia between 4 and 6 weeks of age, which progressed to overt diabetes

during the next 5–6 weeks until they died (Figure 2a). To determine whether the *Irs2* transgene prevented diabetes in the *Irs2−/−* mice, we crossed *rip9→Irs2* or *rip13→Irs2* mice with *Irs2−/−* mice. As expected, transgenic *Irs2* was expressed at a low level in *Irs2−/−:rip9→Irs2* islets and at a high level in *Irs2−/−:rip13→Irs2* islets (data not shown). *Irs2−/−:rip9→Irs2* mice survived for 24 weeks because hyperglycemia progressed slowly toward diabetes between 10 and 24 weeks of age (Figure 2a). By contrast, glucose levels of *Irs2−/−:rip13→Irs2* mice were normal during the 24-week experiment, revealing a dose effect for β cell *Irs2* expression on glucose homeostasis (Figure 2a).

While *Irs2−/−* mice at 8 weeks of age displayed fasting hyperglycemia (*Irs2−/−*: 189 ± 10 mg/dl; WT: 109 ± 6 mg/dl), *Irs2−/−* mice expressing the transgenic *Irs2* were nearly normal (*Irs2−/−:rip9→Irs2*: 124 ± 9 mg/dl; *Irs2−/−:rip13→Irs2*: 121 ± 8 mg/dl). As previously shown, the *Irs2−/−* mice were severely hyperglycemic during an intraperitoneal glucose challenge (Figure 2b). However, at 8 weeks of age, glucose intolerance was slightly improved in the *Irs2−/−:rip9→Irs2* mice and completely normalized in the *Irs2−/−:rip13→Irs2* mice (Figure 2b). Moreover, the *Irs2−/−:rip13→Irs2* mice survived more than a year after the *Irs2−/−* mice died, displaying low random fed blood glucose levels at 15 months (WT: 121 ± 7 mg/dl; *Irs2−/−:rip13→Irs2*: 94 ± 6 mg/dl).
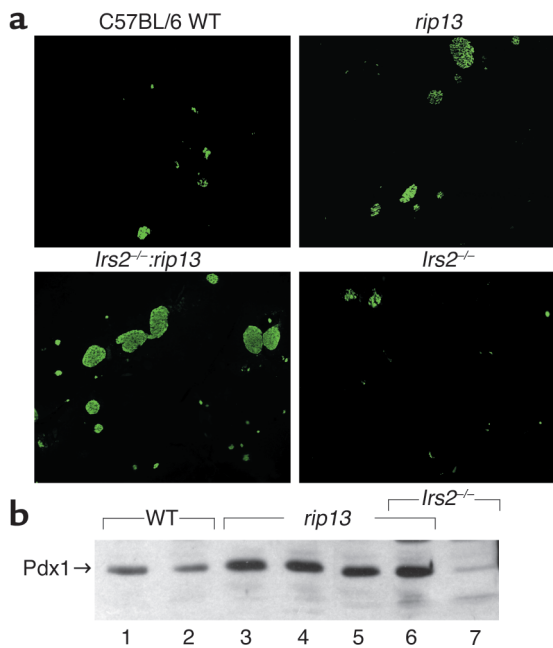
Figure 3
Islet morphometry. (**a**) Insulin immunostaining of representative pancreas sections from 8-week-old C57BL/6 mice and from $rip13^{\rightarrow Irs2}$, $Irs2^{-/-}/rip13^{\rightarrow Irs2}$, and $Irs2^{-/-}$ mice (original magnification, ×100). (**b**) Western blot of Pdx1 protein expression in isolated islets from 4-week-old male mice of the indicated genotypes. Each lane was loaded with 100 µg of total islet protein from one animal and is representative of at least three independent experiments.

$Irs2^{-/-}$ mice are insulin resistant as a result of reduced insulin action in liver, fat, and muscle (9, 22). Before diabetes developed at 6 weeks, serum insulin levels were equally elevated in $Irs2^{-/-}$, $Irs2^{-/-}:rip9^{\rightarrow Irs2}$, and $Irs2^{-/-}:rip13^{\rightarrow Irs2}$ mice to compensate for insulin resistance (Figure 2c). Insulin levels declined dramatically in $Irs2^{-/-}$ mice at 8 weeks, coinciding exactly with the onset of severe diabetes (Figure 2c). Compensatory insulin secretion in $Irs2^{-/-}:rip9^{\rightarrow Irs2}$ mice gradually declined between 12 and 25 weeks until they died with severe diabetes (Figure 2c). $Irs2^{-/-}:rip13^{\rightarrow Irs2}$ mice never developed diabetes due to persistent compensatory hyperinsulinemia, revealing the graded physiological response to $Irs2$ expression in transgenic β cells func-

tioning in a genetically insulin resistant mouse (Figure 2c and data not shown).

Irs2 promotes β cell development and growth. Our previous work suggests that Irs2 signaling regulates survival of pancreatic β cells (18, 19). Compared with WT mice at 8 weeks of age, islet area in $Irs2^{-/-}$ pancreas sections was reduced about threefold, owing to a slightly reduced density of small islets containing 50% fewer β cells (Figure 3a and Table 1). By contrast, islet area in the $rip13^{\rightarrow Irs2}$ sections increased twofold, mainly due to increased density of normal-sized islets (Table 1). Islet density and the β cell content increased in $Irs2^{-/-}:rip13^{\rightarrow Irs2}$ mice, a change that was also revealed by the increased ratio of β cells to α cells (Table 1).

To determine whether β cells in $Irs2^{-/-}:rip13^{\rightarrow Irs2}$ islets were dividing at a higher rate than those in WT or $rip13^{\rightarrow Irs2}$ islets, we injected 8-week-old mice with the thymidine analogue BrdU to measure mitogenesis. BrdU incorporation into β cells during a 6-hour interval increased three- to fourfold in $Irs2^{-/-}:rip13^{\rightarrow Irs2}$ mice compared with WT or $rip13^{\rightarrow Irs2}$ mice; no BrdU-positive cells were detected in $Irs2^{-/-}$ mice (Table 1). The average β cell size never changed upon expression of the $Irs2$ transgene. Thus, compensatory islet expansion during insulin resistance required Irs2 signaling to increase the number of normal-sized β cells.

The effect of Irs2 upregulation on islet gene expression. A possible mechanism by which Irs2 promotes expansion of β cells is through upregulation of the homeodomain transcription factor $Pdx1$ (also called $Idx1$ and $Ipf1$). $Pdx1$ is critical for development of the pancreas in mice and humans, and its complete disruption blocks pancreas development; in adult β cells, $Pdx1$ promotes normal glucose sensing and insulin secretion, and suppresses apoptosis (18, 23–25). Previous results show that $Pdx1$ expression is nearly lost in $Irs2^{-/-}$ islets, but can be restored by downregulation of $Foxo1$ (10). Pdx1 was detected equally by immunoblotting in WT and $rip9^{\rightarrow Irs2}$ islets (data not shown), whereas it was barely detected in our $Irs2^{-/-}$ islet extracts of equal protein concentration (Figure 3b). Consistent with a specific role for Irs2 in Pdx1 expression, Pdx1 protein was strongly upregulated $rip13^{\rightarrow Irs2}$ in WT and $Irs2^{-/-}$ mice containing the $rip13^{\rightarrow Irs2}$ transgene. (Figure 3b). Since upregulation

Table 1
Islet characteristics

	Islet area (% of total)	Density (islets/mm²)	β cells/islet	β/α	BrdU (%)
WT	2.2 ± 0.3	1.3 ± 0.2	22 ± 2	10.4 ± 0.5	0.7 ± 0.1
$rip13^{\rightarrow Irs2}$	4.3 ± 0.4[A]	2.0 ± 0.2[A]	28 ± 0.2	28 ± 4[B]	0.8 ± 0.1
$Irs2^{-/-}:rip13^{\rightarrow Irs2}$	5 ± 1[B]	1.9 ± 0.3[A]	55 ± 9[B]	46 ± 6[B]	2.5 ± 0.7[B]
$Irs2^{-/-}$	0.6 ± 0.1	1.0 ± 0.2	12 ± 1	6 ± 1	ND

Islet area was determined by point-counting morphometry and number of β cells per islet was calculated from the number of nuclei in insulin-positive cells in each islet. Islet density was determined by counting islets with more than five β cells; the β cell/α cell ratio (β/α) was determined directly by point-counting morphometry from sections immunostained with antibodies against glucagon and insulin. BrdU incorporation analysis was performed on double-labeled sections and is expressed as percentage BrdU-positive β cells. Results are expressed as mean ± SEM of six mice per genotype. [A]$P < 0.01$, [B]$P < 0.001$. ND, not determined.
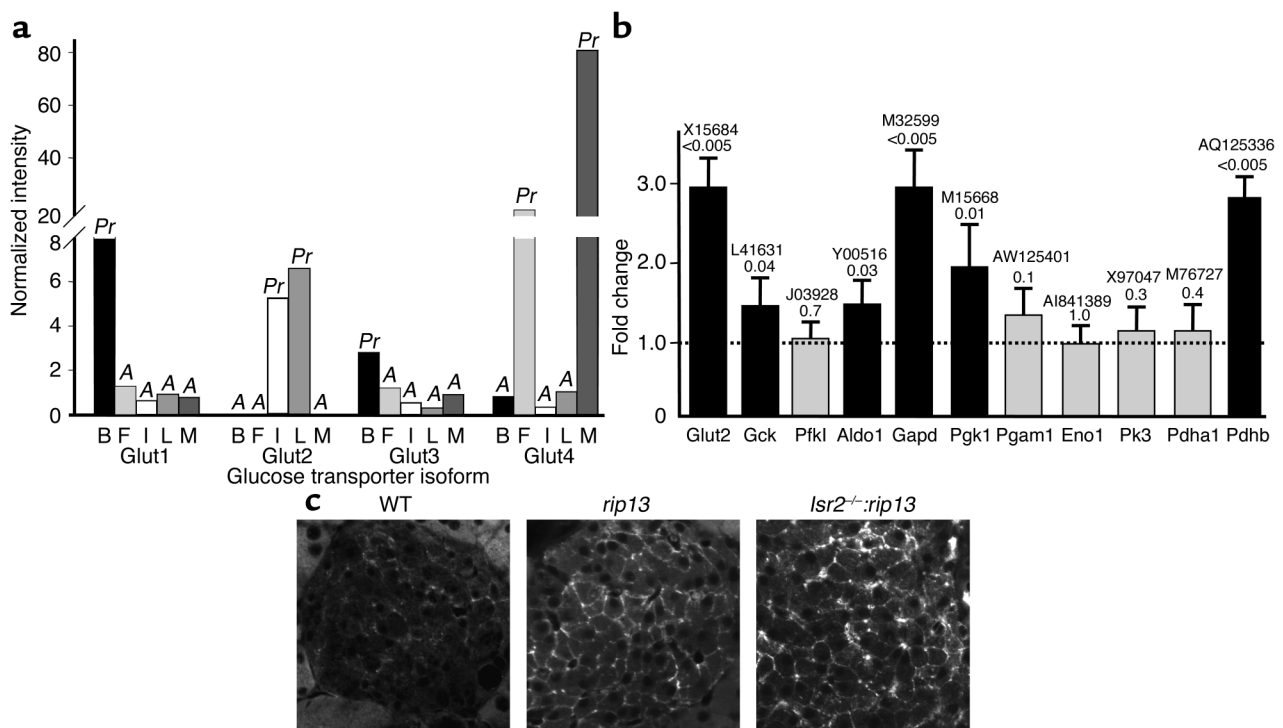
Figure 4
Gene expression in WT tissues and *rip13$^{→Irs2}$* islets. (**a**) Affymetrix MG-U74v2 arrays (A, B, and C arrays) were used to estimate the relative mRNA levels for *Glut1* (93738_at), *Glut2* (103357_at), *Glut3* (93804_at), and *Glut4* (102314_at) in 6-week-old WT brain (B), adipose (F), *rip13$^{→Irs2}$* islets (I), liver (L), and muscle (M); the Affymetrix probe set is indicated in parentheses. Genes called present (*Pr*) or absent (*A*) by GeneChip (version 5) are indicated on the figure. The bars show average of normalized expression measurements obtained from samples of two mice. (**b**) The fold change for mRNA in *rip13$^{→Irs2}$* islets normalized against WT islets is shown for *Glut2*, enzymes of the glycolytic pathway (glucokinase, *Gck*; phosphofructokinase-1, *Pfk1*; aldolase-1, *Aldo1*; GAPDH, *Gapd*; phosphoglycerokinase, *Pgk1*; phosphoglyceromutase-1, *Pgam1*; enolase, *Eno1*; pyruvate kinase, *Pk3*; pyruvate), and the pyruvate dehydrogenase α subunit (*Pdha1*) and β subunit (*Pdhb*). The expression of each gene in *rip13$^{→Irs2}$* islets is reported relative to the normalized level in WT islets; the *P* value for this comparison is indicated. The accession number for each enzyme is indicated above the *P* value. (**c**) Glut2 immunostaining of pancreas sections from 8-week-old WT, *rip13$^{→Irs2}$*, and *Irs2$^{−/−}$:rip13$^{→Irs2}$* mice (original magnification, ×400).

of Pdx1 increases mitogenesis in *Irs2$^{−/−}$* islets, upregulation of *Pdx1* might contribute to the increased number of β cells in *Irs2$^{−/−}$:rip13$^{→Irs2}$* islets (18, 25).

Pdx1 is reported to upregulate the expression of many genes that promote glucose-stimulated insulin secretion, including *Glut2* (26). We used Affymetrix MG-U74v2 arrays to estimate the change in *Glut2* mRNA between WT and *rip13$^{→Irs2}$* islets. The specificity of the *Glut2* probe set was validated against the *Glut1*, *Glut2*, *Glut3*, and *Glut4* probes using samples from *rip13$^{→Irs2}$* islets, brain, fat, liver, and muscle (Figure 4a). As expected, Glut2 was detected in liver and in *rip13$^{→Irs2}$* islets, but absent in the other test tissues; *Glut1* and *Glut3* were restricted to brain; and *Glut4* was expressed exclusively in adipose and muscle tissue (Figure 4a). Compared with WT islets, *Glut2* mRNA increased threefold (*P* < 0.005) in *rip13$^{→Irs2}$* islets (Figure 4b). Immunostaining revealed Glut2 in the plasma membrane of *rip13$^{→Irs2}$* and *Irs2$^{−/−}$:rip13$^{→Irs2}$* β cells, whereas it was barely detected in the plasma membrane of WT islets (Figure 4c). The mRNA for other glycolytic enzymes also increased in *rip13$^{→Irs2}$* islets, including glucokinase (1.5-fold, *P* = 0.04), aldolase-1

(1.5-fold, *P* = 0.03), GAPDH (threefold, *P* < 0.005), and Pgk-1 (1.9-fold, *P* = 0.01); the β subunit of pyruvate dehydrogenase was also increased threefold (*P* < 0.005) (Figure 4b). Identical results were found for *Irs2$^{−/−}$:rip13$^{→Irs2}$* islets. Since the secretion of insulin is tightly coupled to the rate of glucose metabolism, increased activity of glycolytic enzymes is consistent with improved β cell function (27).

Irs2 in β cells prevents diabetes in obese and old mice. Peripheral insulin resistance develops during obesity and aging in mice and people, and progresses to diabetes when β cells fail to compensate with increased insulin secretion (28). To determine whether expression of *Irs2* in β cells promotes compensation for obesity-induced diabetes, WT C57BL/6 mice or *rip13^{Irs2}* mice were weaned and maintained for 60 days on a low- or a high-fat diet. Mice fed the high-fat diet were obese at 12 weeks of age (C57BL/6: 36.5 ± 2.7 g, *n* = 6; *rip13$^{→Irs2}$*: 37.3 ± 2.5 g, *n* = 6) compared with those eating a low-fat diet (C57BL/6: 24.6 ± 2.8 g, *n* = 6; *rip13$^{→Irs2}$*: 25.4 ± 2.6 g, *n* = 6). Obese mice displayed fasting hyperglycemia (obese C57BL/6: 206 ± 16 mg/dl; lean C57BL/6: 101 ± 18 mg/dl) and glucose intolerance (Figure 4a). By
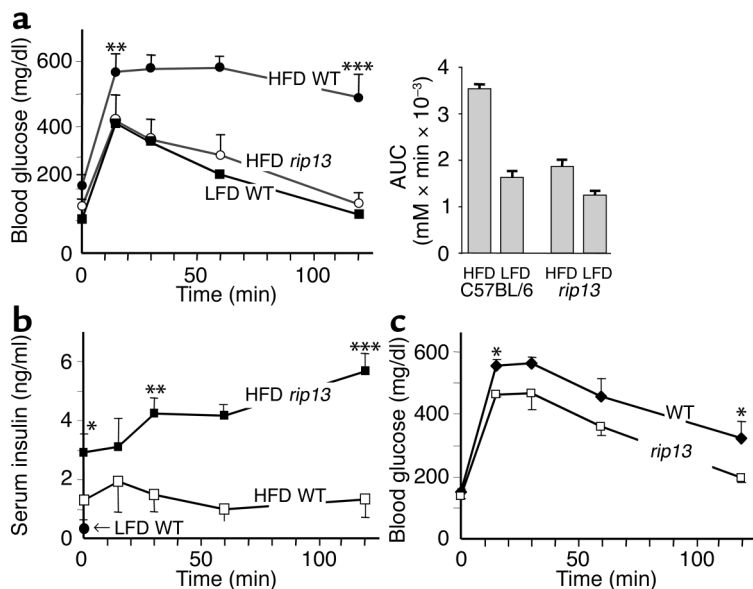
Figure 5

Metabolic characterization of WT and *rip13*→*Irs2* mice maintained on a low-fat diet (LFD) or high-fat diet (HFD). (**a**) An intraperitoneal glucose tolerance test (2 g D-glucose per kg body wt) was performed on fasted C57BL/6 WT or *rip13*→*Irs2* mice maintained on a high-fat or low-fat diet for 60 days after weaning. Blood samples were taken at the timepoints indicated and glucose levels were determined as described. Results are expressed as mean ± SEM of six WT and six *rip13*→*Irs2* male mice (**P < 0.01, ***P < 0.001). (**b**) Serum insulin levels for the indicated timepoints during a glucose tolerance test. Data are the mean values ± SEM (*P < 0.05, **P < 0.01, ***P < 0.001). (**c**) Glucose tolerance test in 6-month-old C57BL/6 WT and *rip13*→*Irs2* mice. Data are the mean values ± SEM of eight mice per genotype (*P < 0.05).

contrast, obese *rip13^Irs2* mice had statistically normal fasting glucose levels (129 ± 15 mg/dl) and normal glucose tolerance (Figure 5a). Consistent with these results, fasting hyperinsulinemia was greater in obese *rip13^Irs2* mice than in obese C57BL/6 WT mice, and during the intraperitoneal glucose challenge insulin levels increased significantly in obese *rip13*→*Irs2* mice but not in obese C57BL/6 WT mice (Figure 5b).
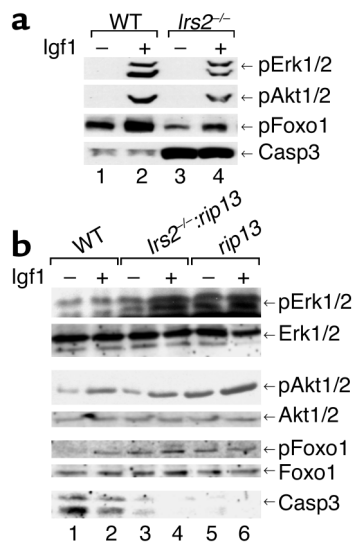
Irs2 expression falls as mice age (10). At 6 months, C57BL/6 mice on a normal diet developed mild glucose intolerance, whereas the *rip13*→*Irs2* mice were normal (Figure 5c). At 40 weeks, islet area was 3.1% ± 0.6% in WT mice, 6% ± 1% in *rip9*→*Irs2* mice, and 10% ± 2% in *rip13*→*Irs2* mice, revealing a graded response to a low and high level of *Irs2* expression. Thus, transgenic *Irs2*–mediated β cell expansion compensates for insulin resistance that develops during aging.

Irs2 promotes β cell survival signaling. Acute or chronic stress and autoimmune responses upregulate proinflammatory cytokines (including TNF-α, IL-1β, and IFN-γ) that promote destruction of β cells at least in part by contributing to apoptosis (29–32). By contrast, Irs protein signaling promotes cell growth and inhibits apoptosis in various cellular backgrounds (19).

In isolated WT murine islets, IGF1 stimulated phosphorylation of Erk1/2, Akt, and the Akt target Foxo1 (Figure 6a). By contrast, in *Irs2*−/− islets the phosphorylation of these targets was reduced, and cleaved/activated caspase-3 accumulated and was insensitive to IGF1 stimulation, which is consistent with decreased growth and survival of *Irs2*−/− β cells (Figure 6a). To determine whether upregulation of *Irs2* restores these signals, islets were isolated from WT mice, or *Irs2*−/−:*rip13*→*Irs2* and *rip13*→*Irs2* mice, cultured for 12 hours, and stimulated with IGF1. IGF1 stimulated phosphorylation of Erk1/2, Akt, and Foxo1 in WT islets; however, the basal and IGF1-stimulated phosphorylation of these proteins was significantly increased in *Irs2*−/−:*rip13*→*Irs2* and *rip13*→*Irs2* islets (Figure 6b). Moreover, upregulation of Irs2 eliminated the accumulation of cleaved cascpase-3, even before IGF1 stimulation, suggesting that Irs2 signaling plays a critical role in β cell survival (Figure 6b).

Figure 6

IGF1 and insulin signaling in isolated islets. (**a**) Islets were isolated from WT or *Irs2*−/− C57BL/6 mice and incubated overnight before stimulation with insulin or IGF1 for 20 minutes as described in Methods. Each lane was loaded with 100 μg of total islet protein. The results are representative of at least three independent experiments. (**b**) Islets were isolated from WT, *Irs2*−/−:*rip13*→*Irs2*, and *rip13*→*Irs2* mice and incubated overnight before stimulation with IGF1 for 20 minutes as described in Methods. The same amount of total protein (300 μg) was loaded onto the gel and transferred to a nitrocellulose membrane. Membranes were analyzed for the presence of Erk1/2 and phosphorylated Erk (pErk1/2); Akt1/2 and phosphorylated Akt (pAkt1/2); Foxo1 and phosphorylated Foxo1 (pFoxo1); and cleaved caspase-3 (Casp3).
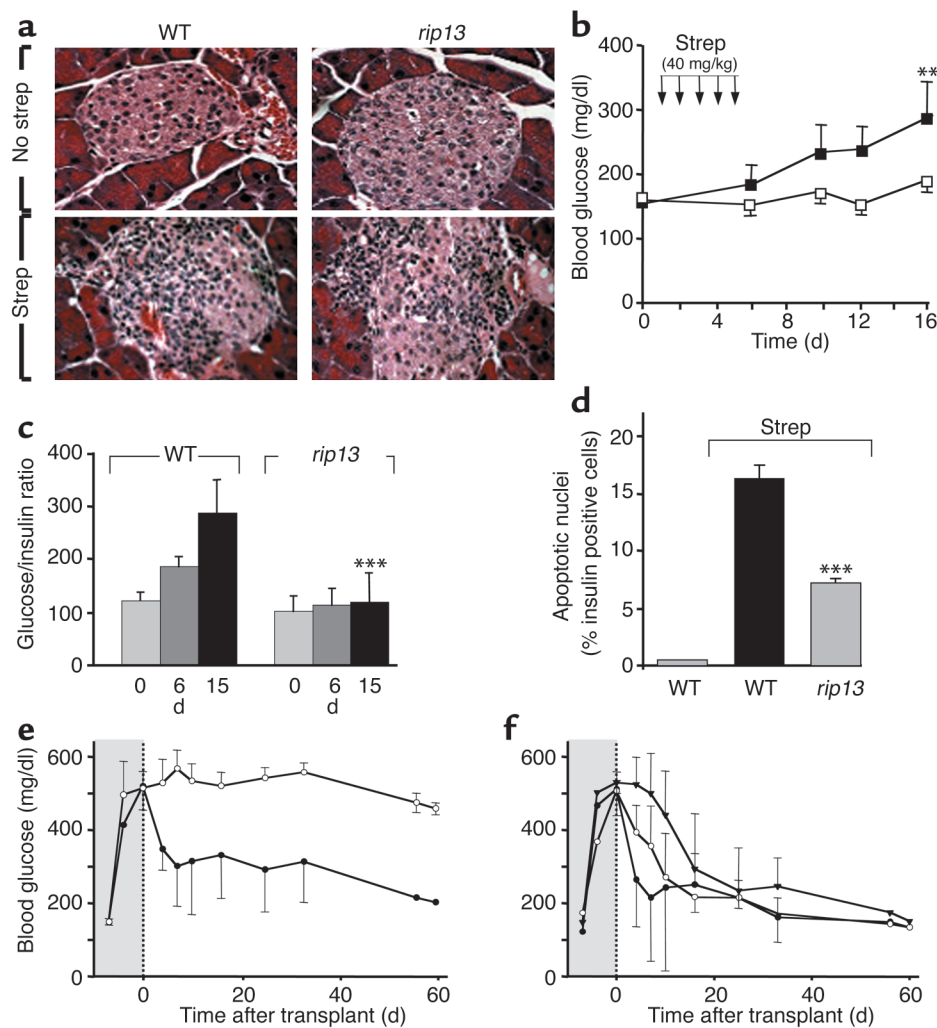
Figure 7

Survival and function of *rip13→Irs2* mice during streptozotocin-induced diabetes. (**a**) Representative H&E-stained pancreas sections from untreated WT or *rip13Irs2* islets compared with pancreas sections obtained 15 days after one injection per day for 5 days of low-dose (40 mg/kg) streptozotocin (strep; original magnification, ×200). (**b**) Blood glucose levels in WT or *rip13→Irs2* mice were measured before and after five (daily) injections of low-dose (40 mg/kg) streptozotocin. Results are expressed as mean ± SEM of eight WT and eight *rip13→Irs2* mice (**P < 0.01); (**c**) Glucose levels (mg/dl) divided by serum insulin levels (ng/dl) are shown for experimental days 0, 6, and 15 (***P < 0.001). (**d**) Apoptotic cells were detected in deparaffinized sections using a rhodamine DNA fragmentation detection assay. The number of apoptotic nuclei per β cell is shown for day 15. Values are expressed as mean ± SEM of eight WT and eight transgenic mice (***P < 0.001). (**e**) Transplantation of WT islets into streptozotocin-diabetic mice. C57BL/6 mice were treated with 100 mg/kg streptozotocin for 3 consecutive days. Blood glucose levels were measured in samples obtained through tail bleeds of fed mice before transplantation (shaded area) and at the indicated ages after transplantation of 300 (filled circles) or 150 (open circles) WT islets. (**f**) Transplantation of *rip13→Irs2* islets into streptozotocin-diabetic mice was conducted in identical fashion with 250 (filled circles), 120 (open circles), or 50 (inverted triangles) islets. Values are mean ± SEM of at least three mice per experiment.

Apoptosis and function of rip13→Irs2 islets transplanted in mice. Since recombinant *Irs2* dramatically reduced the level of cleaved caspase-3, we reasoned that β cell apoptosis might be reduced in *rip13→Irs2* islets. We induced β cell apoptosis in situ by injecting a low dose of streptozotocin for 5 consecutive days into 8-week-old WT or *rip13→Irs2* mice with comparable body weight (21.7 ± 3 g) and comparable levels of random-fed serum glucose (158 ± 11 mg/dl) and plasma insulin (255 ± 60 pmol/l). Blood glucose and serum insulin levels were measured before streptozotocin injection and 6, 12, and 15 days after the first streptozotocin injection. At 15 days, T cell infiltration was comparable in C57BL/6 WT and *rip13→Irs2* mice (Figure 7a). However, low-dose streptozotocin caused insulinopenic diabetes in C57BL/6 WT mice, whereas the *rip13→Irs2* mice were normal (Figure 7, b and c). Apoptotic β cells were readily detected in WT mice, but apoptosis was reduced more than 50% in *rip13→Irs2* mice (Figure 7d). Thus, transgenic *Irs2* prevented the onset of diabetes 15 days after streptozotocin injection, at least in part by suppressing β cell apoptosis.

To test whether *rip13→Irs2* islets are resistant to the effects of stress induced by transplantation, WT or *rip13→Irs2* islets were transplanted under the kidney

capsule of streptozotocin-diabetic mice. In this experiment, 8-week-old C57BL/6 mice were treated with 100 mg/kg streptozotocin for 3 consecutive days to cause severe diabetes (Figure 7, e and f). Without islet transplantation, the diabetic mice died about 10 days after the first injection. By contrast, transplantation of 300 WT islets (>10,000 islets/kg) normalized random-fed glucose levels by 50% within 3–5 days, and glucose levels were nearly normal 60 days later when the experiment was terminated (Figure 7e). By contrast, transplantation of 150 WT islets prevented death but failed to normalize glucose levels (Figure 7e), whereas 80 islets were completely ineffective as the diabetic mice died (not shown). Importantly, 50 $rip13^{\rightarrow Irs2}$ islets (β cell mass equivalent to 80 WT islets) normalized random-fed glucose levels by 50% after 20 days, and quicker treatment was obtained with 120 and 250 $rip13^{\rightarrow Irs2}$ islets (Figure 7f). BrdU incorporation measured in the islet grafts 60 days after transplantation revealed that DNA synthesis was twofold greater in $rip13^{\rightarrow Irs2}$ islets (2.12% ± 0.32% BrdU positive β cells, n = 3) than in WT islets (1.2% ± 0.2% BrdU positive β cells, n = 3). Thus, upregulation of Irs2 in transplanted β cells significantly reduced the number of islets needed to cure diabetes in mice, at least in part by promoting proliferation.

Discussion

The primary cause of type 2 diabetes is unknown; however, there is general agreement that insulin resistance is an early event in the onset of the disease (2, 33). Many insulin-resistant patients secrete sufficient insulin for many years before β cell function fails to compensate and type 2 diabetes emerges (2, 34, 35). Systemic failure of $Irs2$ in mice causes peripheral insulin resistance followed by β cell failure and diabetes, although the time interval is compressed relative to human type 2 diabetes (36). Here we show that upregulation of $Irs2$ exclusively in β cells promotes glucose tolerance in old mice and prevents diabetes in $Irs2^{-/-}$ and obese mice. Moreover, IRS2 protects β cells from destruction by streptozotocin and improves the function of isolated β cells used for transplantation. Thus, upregulation of $Irs2$ in β cells might be a common mechanism to prevent or treat many forms of diabetes.

Massive destruction of β cells is well known in type 1 diabetics, and human autopsy studies reveal that β cell mass is reduced at least 50% in obese patients with type 2 diabetes (37, 38). Thus, insufficient β cell mass relative to peripheral requirements might be a key pathogenic factor of both types of diabetes (38). One way to preserve β cell mass is to reduce apoptosis (25, 39). Streptozotocin in multiple low doses induces β cell apoptosis and diabetes in mice and other mammals, at least in part by promoting T cell infiltration that promotes the production of TNF-α and IFN-γ in the pancreas (40, 41). Upregulation of $Irs2$ in mouse β cells does not reduce T cell infiltration during streptozotocin treatment; however, it reduces apoptosis of β cells

by 50%, and prevents the onset of diabetes for at least 15 days. Several pathways promote survival of β cells, and many of these mechanism are mediated by insulin/IGF1 → Irs2 signaling (19). Moreover, Irs2 signaling mediates the phosphorylation of Bad and the forkhead transcription factor Foxo1, which control important survival pathways (42, 43). The activation of Akt is an important mechanism used by insulin and IGF1 to inhibit apoptosis in a variety of cellular environments (44). Recent results suggest that Akt2 might promote β cell survival by linking Irs2 to Foxo1, especially during cytokine-induced stress (8).

Phosphorylated Bad dissociates from the antiapoptotic protein Bcl2, which inhibits activation of the caspase cascade, including the accumulation of the cleaved/activated effector caspase-3, which promotes apoptosis (42). IGF1 or insulin stimulation ordinarily inhibits the accumulation of cleaved/activated caspase-3 through activation of Akt; however, insulin- and IGF1-stimulated Akt phosphorylation is reduced in $Irs2^{-/-}$ islets, increasing the accumulation of cleaved/activated caspase-3 that promotes β cell apoptosis (19). IGF1 stimulation weakly reduces the levels of cleaved/activated caspase-3 in our WT isolated islets, consistent with low or undetectable Irs2 levels following overnight incubations. However, transgenic upregulation of $Irs2$ almost completely blocks the accumulation of activated caspase-3, even before addition of exogenous IGF1. Thus, Irs2 is an important inhibitor of caspase-mediated apoptosis.

Foxo1 is an important Akt substrate that links insulin/IGF signaling to gene regulation (43). Phosphorylated Foxo1 is ordinarily excluded from the nucleus, which changes the expression of various genes including the upregulation of $Pdx1$ (10). $Pdx1$ plays an important role in gut and β cell development, and promotes glucose sensing and insulin secretion in adult β cells (45–47). Partial $Pdx1$ deficiency leads to an organ-level defect in insulin secretion and diabetes (25). Transgenic upregulation of $Foxo1$ constitutively increases the level of nuclear Foxo1, which downregulates $Pdx1$ and impairs β cell function (10). By contrast, reduced expression of $Pdx1$ in $Irs2^{-/-}$ islets is consistent with nuclear accumulation of dephosphorylated Foxo1, whereas increased $Pdx1$ levels in $Irs2^{-/-}:Foxo1^{+/-}$ islets reflect the reduced content of cellular Foxo1 (10). Similarly, upregulation of $Irs2$ in $rip13^{\rightarrow Irs2}$ or $Irs2^{-/-}:rip13^{\rightarrow Irs2}$ β cells increases Foxo1 phosphorylation to promote its exclusion from the nucleus, which is consistent with elevated $Pdx1$. Thus, $Pdx1$ might mediate many of the effects of $Irs2$ in β cells, as transgenic upregulation of $Pdx1$ restores β cell function and promotes normal glycemia in $Irs2^{-/-}$ mice (18). Interestingly, $Pdx1$ expression persists in some lines of C57BL/6 mice lacking $Irs2$, which protects them from diabetes (48).

Whether Irs2 signaling promotes β cell growth is difficult to determine. Before birth, Irs2 signaling is not required for β cell development, as $Irs2^{-/-}$ neonates have sufficient islet function to avoid diabetes for the

first 8 weeks of life. However, β cell mass fails to expand in *Irs2*^{−/−} mice even though peripheral insulin resistance is expected to promote expansion as it does in *Irs1*^{−/−} mice (9). Alone, upregulation of *Irs2* does not increase mitogenesis in β cells; however, islet density increases equally in both *rip13*[→Irs2] and *Irs2*^{−/−}:*rip13*[→Irs2] mice. Alternatively, BrdU labeling is detectable in *Irs2*^{−/−}:*rip13*[→Irs2] mice, suggesting that insulin resistance mediates β cell mitogenesis through Irs2 signaling. Unfortunately, our experiments do not reveal the mechanism by which *Irs2* increases islet density. However, Kitamura et al. suggest that nuclear exclusion of Foxo1 from ductal precursors might promote the formation of new duct-associated islets by upregulating *Pdx1* (10). Thus, relative hyperinsulinemia during the initial response to insulin resistance might promote Irs2-mediated β cell growth. Unfortunately, this mechanism is expected to eventually fail, as Irs2 signaling diminishes during progressive insulin resistance.

Although our work focuses on murine β cells, preliminary experiments show that upregulation of *IRS2* in isolated human islets by adenoviral-mediated infection increases glucose-stimulated insulin release and BrdU incorporation (data not shown). Thus, pharmacologic or genetic approaches that upregulate *Irs2* in β cells or promote Irs2-mediated downstream signals, such as reduction of nuclear Foxo1, might also improve β cell function in people. Tools to upregulate *Irs2* have not been available because the regulation of *Irs2* gene expression is poorly studied. However, results with HeLa cells suggest that human *IRS2* is moderately upregulated by cAMP and strongly upregulated by progesterone or the combination of cAMP and RU486 (49).

In our experiments, glucagen-like peptide 1, exendin-4 or dibutyl-cAMP strongly upregulated Irs2 protein in Min6 β cells, and similar results were observed with isolated human islets (data not shown). A mechanism for the regulation of *Irs2* by cAMP was recently suggested by Jhala et al., who demonstrated a functional CRE in the murine *Irs2* gene (21). Thus, the trophic effect of GLP1/exendin-4 in rodents and people might be explained, at least in part, by the upregulation of IRS2 (50, 51). GLP1 secretion decreases in people with type 2 diabetes, but subcutaneous administration of GLP1 improves glucose homeostasis; lowers body weight, hemoglobin A(1C), and free fatty acids; and increases insulin sensitivity and insulin action (52, 53). Moreover, GLP1/exendin-4 inhibits both cytokine and fatty acid–induced apoptosis in β cells, and delays the development of diabetes in Zucker diabetic fatty rats by reducing β cell loss (54). Since these changes are also expected upon increased Irs2 protein levels, GLP1/exendin-4 or other β cell–specific cAMP agonists might prevent β cell failure by promoting Irs2 signaling.

As absolute or relative insulin insufficiency is associated with all forms of diabetes, β cell replacement via transplantation represents an attractive alternative for treating human diabetics; however, the isolation of sufficient (at least 10,000 islets/kg) high-quality human islets that survive and function after transplantation is challenging (55). Given the capacity of the *rip13*[→Irs2] transgene to preserve or enhance β cell function during transplantation in mice, upregulation of *IRS2* by pharmacologic or genetic approaches just before transplantation might improve the function of human islets and reduce the number needed for successful transplantation.

In summary, upregulation of *Irs2* in β cells disrupts disease progression in mice, and if expressed highly enough, can prevent the onset of diabetes caused by *Irs2* disruption or diet-induced obesity. The Irs2 signaling system includes many elements that propagate the insulin/IGF signal to cytoplasmic regulatory enzymes and to nuclear regulatory elements. In β cells, this includes certain MODY genes, revealing an intriguing link between insulin signaling and autosomal early onset diabetes (10, 18). Further investigation of the Irs2 branch of the insulin/IGF signaling cascade might explain the relationship between β cell failure and peripheral insulin resistance that causes type 2 diabetes. If the IRS2 signaling cascade is a master regulator that integrates β cell function with peripheral insulin action, upregulation of IRS2 by nutritional, pharmacologic, or genetic intervention could be a general way to slow progression or prevent the onset of diabetes.

1. Zimmet, P., Alberti, K.G., and Shaw, J. 2001. Global and societal implications of the diabetes epidemic. *Nature.* **414**:782–787.
2. Taylor, S.I., Accili, D., and Imai, Y. 1994. Insulin resistance or insulin deficiency. Which is the primary cause of NIDDM? *Diabetes.* **43**:735–740.
3. Kahn, S.E. 2003. The relative contributions of insulin resistance and beta-cell dysfunction to the pathophysiology of type 2 diabetes. *Diabetologia.* **46**:3–19.
4. Ehrmann, D.A., et al. 2002. Insulin secretory responses to rising and falling glucose concentrations are delayed in subjects with impaired glucose tolerance. *Diabetologia.* **45**:509–517.
5. Kitamura, T., Kahn, C.R., and Accili, D. 2003. Insulin receptor knockout mice. *Annu. Rev. Physiol.* **65**:313–332.
6. Yenush, L., and White, M.F. 1997. The IRS-signalling system during insulin and cytokine action. *Bioessays.* **19**:491–500.
7. Kido, Y., Nakae, J., and Accili, D. 2001. Clinical review 125: the insulin receptor and its cellular targets. *J. Clin. Endocrinol. Metab.* **86**:972–979.
8. Garofalo, R.S., et al. 2003. Severe diabetes, age-dependent loss of adipose tissue, and mild growth deficiency in mice lacking Akt2/PKBβ. *J. Clin. Invest.* **112**:197–208. doi:10.1172/JCI200316885.
9. Withers, D.J., et al. 1998. Disruption of IRS-2 causes type 2 diabetes in mice. *Nature.* **391**:900–904.
10. Kitamura, T., et al. 2002. The forkhead transcription factor *Foxo1* links insulin signaling to *Pdx1* regulation of pancreatic β cell growth. *J. Clin. Invest.* **110**:1839–1847. doi:10.1172/JCI200216857.
11. Kulkarni, R.N., et al. 2002. beta-cell-specific deletion of the Igf1 receptor leads to hyperinsulinemia and glucose intolerance but does not alter beta-cell mass. *Nat. Genet.* **31**:111–115.
12. Kulkarni, R.N., et al. 1999. Tissue-specific knockout of the insulin receptor in pancreatic β cells creates an insulin secretory defect similar to that in type 2 diabetes. *Cell.* **96**:329–339.
13. Xuan, S., et al. 2002. Defective insulin secretion in pancreatic β cells lacking type 1 IGF receptor. *J. Clin. Invest.* **110**:1011–1019. doi:10.1172/JCI200215276.
14. Bonner-Weir, S. 2000. Islet growth and development in the adult. *J. Mol. Endocrinol.* **24**:297–302.

15. Avruch, J. 1998. A signal for b-cell failure. *Nature.* **391**:846–847.

16. Ehrmann, D.A., Tang, X., Yoshiuchi, I., Cox, N.J., and Bell, G.I. 2002. Relationship of insulin receptor substrate-1 and -2 genotypes to phenotypic features of polycystic ovary syndrome. *J. Clin. Endocrinol. Metab.* **87**:4297–4300.

17. Sutton, R., Peters, M., McShane, P., Gray, D.W., and Morris, P.J. 1986. Isolation of rat pancreatic islets by ductal injection of collagenase. *Transplantation.* **42**:689–691.

18. Kushner, J.A., et al. 2002. Pdx1 restores beta cell function in Irs2 knockout mice. *J. Clin. Invest.* **109**:1193–1201. doi:10.1172/JCI200214439.

19. Withers, D.J., et al. 1999. Irs-2 coordinates Igf-1 receptor-mediated beta-cell development and peripheral insulin signalling. *Nat. Genet.* **23**:32–40.

20. Flier, S.N., Kulkarni, R.N., and Kahn, C.R. 2001. Evidence for a circulating islet cell growth factor in insulin-resistant states. *Proc. Natl. Acad. Sci. U. S. A.* **98**:7475–7480.

21. Jhala, U.S., et al. 2003. cAMP promotes pancreatic beta-cell survival via CREB-mediated induction of IRS2. *Genes Dev.* **17**:1575–1580.

22. Previs, S.F., Withers, D.J., Ren, J.M., White, M.F., and Shulman, G.I. 2000. Contrasting effects of IRS-1 vs. IRS-2 gene disruption on carbohydrate and lipid metabolism in vivo. *J. Biol. Chem.* **275**:38990–38994.

23. Jonsson, J., Carlsson, L., Edlund, T., and Edlund, H. 1994. Insulin-promoter-factor 1 is required for pancreas development in mice. *Nature.* **371**:606–609.

24. Stoffers, D.A., Zinkin, N.T., Stanojevic, V., Clarke, W.L., and Habener, J.F. 1997. Pancreatic agenesis attributable to a single nucleotide deletion in the human IPF1 gene coding sequence. *Nat. Genet.* **15**:106–110.

25. Johnson, J.D., et al. 2003. Increased islet apoptosis in $Pdx1^{+/-}$ mice. *J. Clin. Invest.* **111**:1147–1160. doi:10.1172/JCI200316537.

26. Ahlgren, U., Jonsson, J., Jonsson, L., Simu, K., and Edlund, H. 1998. beta-cell-specific inactivation of the mouse Ipf1/Pdx1 gene results in loss of the beta-cell phenotype and maturity onset diabetes. *Genes Dev.* **12**:1763–1768.

27. Yoon, J.C., et al. 2003. Suppression of beta cell energy metabolism and insulin release by PGC-1alpha. *Dev. Cell.* **5**:73–83.

28. Matthews, D.R., et al. 1985. Homeostasis model assessment: insulin resistance and beta-cell function from fasting plasma glucose and insulin concentrations in man. *Diabetologia.* **28**:412–419.

29. Hammonds, P., et al. 1990. Insulin-secreting beta-cells possess specific receptors for interleukin-1 beta. *Growth Regul.* **261**:97–100.

30. Zumsteg, U., et al. 1993. Differential interleukin-1 receptor antagonism on pancreatic beta and alpha cells. Studies in rodent and human islets and in normal rats. *Diabetologia.* **36**:759–766.

31. Mandrup-Poulsen, T., Bendtzen, K., Dinarello, C.A., and Nerup, J. 1987. Human tumor necrosis factor potentiates human interleukin 1-mediated rat pancreatic beta-cell cytotoxicity. *J. Immunol.* **139**:4077–4082.

32. Suarez-Pinzon, W.L., Strynadka, K., Schulz, R., and Rabinovitch, A. 1994. Mechanisms of cytokine-induced destruction of rat insulinoma cells: the role of nitric oxide. *Endocrinology.* **134**:1006–1010.

33. Shulman, G.I. 2000. Cellular mechanisms of insulin resistance. *J. Clin. Invest.* **106**:171–176.

34. Reaven, G.M. 2002. Multiple CHD risk factors in type 2 diabetes: beyond hyperglycaemia. *Diabetes Obes. Metab.* **4**(Suppl. 1):S13–S18.

35. Reaven, G.M. 2001. Insulin resistance: why is it important to treat? *Diabetes Metab.* **27**:247–253.

36. White, M.F. 2002. IRS proteins and the common path to diabetes. *Am. J. Physiol. Endocrinol. Metab.* **283**:E413–E422.

37. Clark, A., et al. 1988. Islet amyloid, increased A-cells, reduced B-cells and exocrine fibrosis: quantitative changes in the pancreas in type 2 diabetes. *Diabetes Res.* **9**:151–159.

38. Butler, A.E., et al. 2003. Beta-cell deficit and increased beta-cell apoptosis in humans with type 2 diabetes. *Diabetes.* **52**:102–110.

39. Pick, A., et al. 1998. Role of apoptosis in failure of β-cell mass compensation for insulin resistance and β-cell defects in the male Zucker diabetic fatty rat. *Diabetes.* **47**:358–364.

40. Herold, K.C., et al. 1996. Regulation of cytokine production during development of autoimmune diabetes induced with multiple low doses of streptozotocin. *J. Immunol.* **156**:3521–3527.

41. Holstad, M., and Sandler, S. 2001. A transcriptional inhibitor of TNF-alpha prevents diabetes induced by multiple low-dose streptozotocin injections in mice. *J. Autoimmun.* **16**:441–447.

42. Brazil, D.P., and Hemmings, B.A. 2001. Ten years of protein kinase B signalling: a hard Akt to follow. *Trends Biochem. Sci.* **26**:657–664.

43. Tran, H., Brunet, A., Griffith, E.C., and Greenberg, M.E. 2003. The many forks in FOXO's road. *Sci. STKE.* **2003**:RE5.

44. Datta, S.R., et al. 1997. Akt phosphorylation of BAD couples survival signals to the cell-intrinsic death machinery. *Cell.* **91**:231–241.

45. Peers, B., Leonard, J., Sharma, S., Teitelman, G., and Montminy, M.R. 1994. Insulin expression in pancreatic islet cells relies on cooperative interactions between the helix loop helix factor E47 and the homeobox factor STF-1. *Mol. Endocrinol.* **8**:1798–1806.

46. Watada, H., et al. 1996. The human glucokinase gene beta-cell-type promoter: an essential role of insulin promoter factor 1/PDX-1 in its activation in HIT-T15 cells. *Diabetes.* **45**:1478–1488.

47. Waeber, G., Thompson, N., Nicod, P., and Bonny, C. 1996. Transcriptional activation of the GLUT2 gene by the IPF-1/STF-1/IDX-1 homeobox factor. *Mol. Endocrinol.* **10**:1327–1334.

48. Suzuki, R., et al. 2003. Pdx1 expression in Irs2 deficient mouse beta-cells is regulated in a strain-dependent manner. *J. Biol. Chem.* doi:10.1074/jbc.M307004200.

49. Vassen, L., Wegrzyn, W., and Klein-Hitpass, L. 1999. Human insulin receptor substrate-2 (IRS-2) is a primary progesterone response gene. *Mol. Endocrinol.* **13**:485–494.

50. Holst, J.J. 2002. Therapy of type 2 diabetes mellitus based on the actions of glucagon-like peptide-1. *Diabetes Metab. Res. Rev.* **18**:430–441.

51. Li, Y., et al. 2003. Glucagon-like peptide-1 receptor signaling modulates beta cell apoptosis. *J. Biol. Chem.* **278**:471–478.

52. Lugari, R., et al. 2002. Evidence for early impairment of glucagon-like peptide 1-induced insulin secretion in human type 2 (non insulin-dependent) diabetes. *Horm. Metab. Res.* **34**:150–154.

53. Zander, M., Madsbad, S., Madsen, J.L., and Holst, J.J. 2002. Effect of 6-week course of glucagon-like peptide 1 on glycaemic control, insulin sensitivity, and beta-cell function in type 2 diabetes: a parallel-group study. *Lancet.* **359**:824–830.

54. Farilla, L., et al. 2002. Glucagon-like peptide-1 promotes islet cell growth and inhibits apoptosis in Zucker diabetic rats. *Endocrinology.* **143**:4397–4408.

55. Goss, J.A., et al. 2002. Achievement of insulin independence in three consecutive type-1 diabetic patients via pancreatic islet transplantation using islets isolated at a remote islet isolation center. *Transplantation.* **74**:1761–1766.